Plant Soil (2026) 518:543–550
https://doi.org/10.1007/s11104-025-08008-y

RESEARCH ARTICLE

Zinc hyperaccumulation in *Cardamine waldsteinii* from the Western Balkans: a field and synchrotron investigation

Ksenija Jakovljević · Mirko Salinitro · Sandro Bogdanović · Siniša Škondrić · Tomica Mišljenović · Antony van der Ent

Received: 12 July 2025 / Accepted: 13 October 2025 / Published online: 11 November 2025

Abstract

Background and aims Zinc hyperaccumulation is a very rare phenomenon on nature known from only 20 taxa around the World, especially in the genus *Noccaea* (Brassicaceae). *Cardamine waldsteinii* is a recently discovered (hyper)accumulator of zinc from central Europe and the Balkans. This study aimed to determine the ability of zinc hyperaccumulation in wild populations of *C. waldsteinii* and to elucidate its internal distribution in plant organs and tissues.

Methods Plant and associated soils samples from the native habitat of *C. waldsteinii* in the Western Balkans were collected and analysed to determine Zn accumulation. This was coupled with synchrotron micro-X-ray fluorescence elemental imaging, to elucidate the distribution of zinc in the plant organs.

Results The results confirm that *C. waldsteinii* is a genuine zinc hyperaccumulator meeting all established criteria for hyperaccumulation. The endodermis and vascular bundles were the main sites of zinc localisation in the roots and in the stem, whereas in the leaves the marginal areas were the most zinc enriched.

Conclusions We confirm the hyperaccumulation properties of *C. waldsteinii* in wild populations, whilst synchrotron micro-X-ray fluorescence elemental imaging reveal the zinc localisation patterns in organs and tissues. This study highlights the need for a comprehensive study of the genus *Cardamine* with the aim of discovering new metal/metalloid hyperaccumulator species.

Keywords Hyperaccumulator · Elemental localisation · Synchrotron-based X-ray fluorescence imaging

Responsible Editor: Paula Pongrac

K. Jakovljević
Department of Ecology, Institute for Biological Research, Siniša Stanković – National Institute of the Republic of Serbia, University of Belgrade, Belgrade, Serbia

M. Salinitro · A. van der Ent (✉)
Laboratory of Genetics, Wageningen University and Research, Wageningen, The Netherlands
e-mail: antony.vanderent@wur.nl

S. Bogdanović
Department of Agricultural Botany, University of Zagreb Faculty of Agriculture, Zagreb, Croatia

S. Škondrić
Faculty of Natural Sciences and Mathematics, University of Banja Luka, Banja Luka, Bosnia and Herzegovina

T. Mišljenović
Institute of Botany and Botanical Garden, Faculty of Biology, University of Belgrade, Belgrade, Serbia

A. van der Ent
Université de Lorraine, INRAE, 54000 Nancy, LSE, France

Introduction

Cardamine waldsteinii Dyer (Brassicaceae) is a newly discovered Zn accumulator from Central Europe and the Balkans with up to 3050 μg g^{-1} Zn in herbarium material revealed by handheld X-ray fluorescence (XRF) analysis, compared to 2210 μg g^{-1} in the leaves of this species collected in the field (Jakovljević et al. 2023). To date, foliar concentrations of Zn in excess the 3000 μg g^{-1}, which is the nominal threshold for hyperaccumulation of this element (van der Ent et al. 2013), have been found in only approximately 20 taxa globally (Reeves et al. 2018), compared to ~700 plant taxa known to hyperaccumulate metals/metalloids globally (Reeves et al. 2018). Zinc is an essential element for plants, the second most abundant transition metal in plants after Fe (Broadley et al. 2007). It is important for the synthesis of proteins, membrane integrity and detoxification, a cofactor for more than 300 proteins, and is found in all six classes of enzymes (Kaur and Garg 2021).

Weathering of parental rock is the main source of Zn in soil, with availability largely determined by the pH value, being higher in acid soils, and leading to Zn deficiency in calcareous soils (Marschner 2012). Zinc deficiency is acerbated in soils with low organic matter content (Broadley et al. 2007), limiting plant growth and crop yield, up to 30% (Alloway 2009). The average concentrations of Zn in most 'normal' soils range between 10−300 μg g^{-1} (Alloway 2008), but can be in excess of 100,000 μg g^{-1} in rare calamine soils (metalliferous soils highly enriched in Zn, Pb and Cd) (Cappuyns et al. 2006), where most Zn-hyperaccumulator plants occur. However, in a number of species, including *Arabidopsis halleri* (L.) O'Kane & Al-Shehbaz and *Noccaea caerulescens* (J.Presl & C.Presl) F.K.Mey., can attain hyperaccumulation-level of Zn while growing in soils with background concentrations of Zn. In *A. halleri*, concentrations of up to 53,900 μg g^{-1}, the highest Zn foliar concentration recorded to date, was found while it grew in normal soils with only 342 μg g^{-1} Zn (Stein et al. 2017). Similarly, Zn concentrations in the leaves of *N. caerulescens* growing on a soil with only 139 μg g^{-1} Zn reached up to ~9000 μg g^{-1} (Reeves et al. 2001). Similar in *C. waldsteinii* foliar Zn concentration of > 2000 μg g^{-1} were reported in a plant growing on a soil with 66.1 μg g^{-1} Zn (Jakovljević et al. 2023). Apart from Zn hyperaccumulation identified in herbarium specimens of *C. waldsteinii*, trace element hyperaccumulation is rare in other *Cardamine* species, found only in *C. hupingshanensis* K.M.Liu, L.B.Chen, H.F.Bai & L.H.Liu, a hyperaccumulator of selenium (Se) from China (Zhou et al. 2018).

In the current study, we aim to determine the ability of Zn hyperaccumulation in wild populations of *C. waldsteinii* in the Western Balkans. Furthermore, we aim to elucidate the internal distribution of Zn in plant organs of *C. waldsteinii* using synchrotron micro-X-ray fluorescence elemental imaging (μXRF). In particular, we are interested to learn whether the patterns of Zn localisation are different compared to other well-studied Zn hyperaccumulators, such as *Noccaea* spp. and *Sedum plumbizincicola*.

Materials and methods

Collection of samples in the field and processing for elemental analysis

The samples of *C. waldsteinii* (Fig. 1) and the associated rhizospheric soil (the soil around the roots of

Fig. 1 Flowering plant of *Cardamine waldsteinii* growing in its natural habitat on limestone near Mt. Medvednica, Croatia

each collected plants at a depth of ~ 5–10 cm) (n = 3 in SP1–SP7; n = 5 in SP8–SP12) were collected from localities in Croatia and Bosnia and Herzegovina, representing the core of the species distribution area (Sabovljević et al. 2025). The additional sample, cultivated at the Loki Schmidt Botanical Garden in Hamburg, Germany, was collected for the synchrotron μXRF analysis. The details on the collection localities are provided in Fig. 2. After initial air-drying in the field, the plant samples were oven-dried at 60 °C for 5 days and subjected to a thorough cleaning to remove the superficial dust with hexane washing according to the protocols of Reeves and Kruckeberg (2018) and Paul et al. (2019). In short, the plant material samples (~ 1 g) was immersed in 20 mL of anhydrous hexane (HPLC-grade, ≥ 95%, Sigma-Aldrich) in 50 mL polypropylene tubes, subjected to sonication, extracted from the hexane and dried prior powdering. The plant material was ground to a fine powder (< 200 μm) in an impact mill (IKA TubeMill 100 Control). The soil samples were air-dried for 4 days until constant weight and sieved to < 500 μm using a stainless mesh screen (Royal Eijkelkamp Sieve Set Ø 200 mm).

Elemental analysis of plant and soil material samples

For the bulk monochromatic X-ray fluorescence (MXRF) analysis, powdered plant material (0.3 g subsamples) was placed into custom MXRF sample holders and covered with 6.0 μm thin polypropylene film (Chemplex Industries Inc.), while sieved 0.2 g subsamples of the soil were placed in custom XRF sample holders and covered with an 6.0 μm thin polypropylene film (Chemplex Industries Inc.). The MXRF analysis of the plant and soil powdered material were performed using a Z-Spec JP500 instrument (Z-Spec Inc.) in 'Plant' and 'Soil' mode, respectively (Kahlon et al. 2024; Zhang et al. 2025). These modes

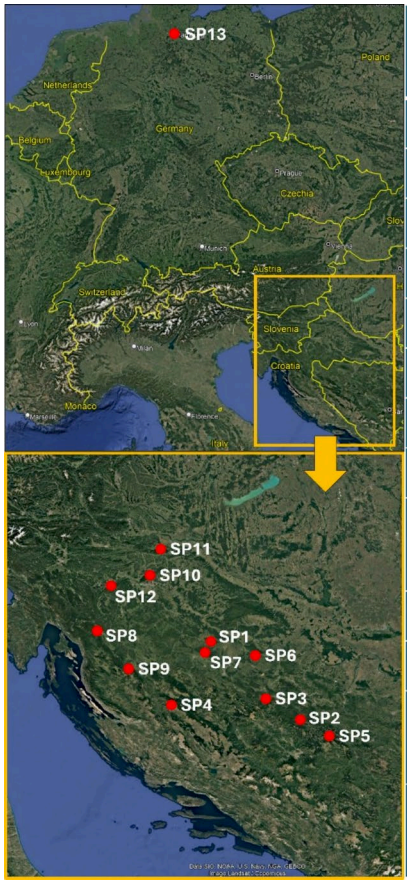

Sampling point	Country	Locality	Altitude (m a.s.l.)	Latitude (°)	Longitude (°)
SP1	Bosnia and Herzegovina	Prosara, Medjedja	127	45.1957	16.9584
SP2	Bosnia and Herzegovina	Banovići, Željova River	447	44.3654	18.4488
SP3	Bosnia and Herzegovina	Teslić, Vrućica Spa	326	44.5894	17.8862
SP4	Bosnia and Herzegovina	Klekovača, Oštrelj	1083	44.4798	16.4092
SP5	Bosnia and Herzegovina	Vlasenica, Cvijetanj	511	44.1988	18.9095
SP6	Bosnia and Herzegovina	Motajica, Osovica	208	45.0472	17.7066
SP7	Bosnia and Herzegovina	Kozara, Moštanica	373	45.0632	16.8827
SP8	Croatia	Velika Kapela, Klek	661	45.2447	15.1489
SP9	Croatia	Plitvice, Prijeboj-Ličko Petrovo Selo	643	44.8567	15.6926
SP10	Croatia	Medvednica Nature Park	852	45.8868	15.9282
SP11	Croatia	Mt Ivanščica	815	46.1942	16.1047
SP12	Croatia	Žumberak-Samoborsko Gorje Nature Park	980	45.7503	15.3115
SP13	Germany	Loki Schmidt Botanical Garden, Hamburg	48	53.5660	9.8606

Fig. 2 Distribution and characterisation of sample points (SP) of *Cardamine waldsteinii*

utilize different Fundemental Parameters in the equation used to convert raw fluorescence counts to concentration values expressed in μg g^{-1}. This equation takes into account bulk composition, density and thickness of the sample. This instrumentation uses monochromatic X-ray fluorescence excitation at 17.48 keV to analyse elements Z = 13 (Al) to Z = 40 (Zr) on the K-lines and up to Z = 92 (U) on the L-lines with optimum sensitivity for elements Cu–Se and Hg-Tl-Pb with LODs ranging from 0.009–0.025 μg g^{-1}. Quality controls included NIST SRM 1570a Trace elements in spinach leaves and NIST SRM 1573a Tomato leaves.

Synchrotron μXRF elemental imaging

Cardamine waldsteinii only flowers and bares leaves for a short time in spring and the large distance travelling between wild localities where it occurs in Bosnia and Herzegovina and Croatia, and the synchrotron facility in Hamburg, made it impossible to get live samples from a natural population. However, *C. waldsteinii* is cultivated on normal (*i.e.,* not Zn-enriched soil) soil at the Loki Schmidt Botanical Garden in Hamburg. Therefore, a live plant specimen was collected from this locality and used for the synchrotron μXRF elemental imaging described below. The synchrotron micro-X-ray fluorescence (μXRF) experiments were performed at PETRA III (Deutsches Elektronen-Synchrotron DESY), a 6 GeV synchrotron radiation source, specifically at the hard X-ray microprobe undulator beamline P06 (Boesenberg et al. 2016). This beamline is equipped with a cryogenically cooled double-crystal monochromator with Si(111) crystals and using different focusing optics, the X-ray beam can be focused down to sub-micron level. An ion chamber upstream of the sample is used to monitor the incoming flux, while a 500 μm thick Si PIPS diode with an active area of 19 mm diameter (PD300-500CB, Mirion Technologies (Canberra) GmbH, Germany) located downstream of the sample can be used to record the transmitted X-ray intensity to obtain absorption data. Multiple XRF detectors enable the measurement of X-ray fluorescence data. The incident X-ray energy was 15 keV for the entire experiment and focussed with K-B mirrors to 2.1 × 1.0 μm (h × v) with prefocusing, resulting in a flux of ~1.0^{11} ph/s in the focus. For XRF detection, both a Vortex ME4 (4 elements) in 45° geometry and Vortex ME (1 element, 2 mm thick) in 315° geometry with Xspress3 pulse processors were used. The live plant specimen from the Loki Schmidt Botanical Garden was used to elemental maps of whole plant organs. These were excised and directly mounted between two sheets of thin film (4.0 μm thickness) stretched over a 3D printed plastic frame holder to prevent dehydration during the measurement. Thin sections of the root, stem, and petiole were made by hand cutting with a new stainless steel razor blade for each specimen. This 'dry knife' method allow to obtain 0.2–0.5 mm thick sections without any chemical fixing, embedding or water immersion; thereby avoiding elemental deportment. The sections were immediately lifted from the razorblade with a fine-tip brush and deposited onto thin film (Ultralene® Window Film) of 4.0 μm thickness (Cole-Parmer SamplePrep 3525) stretched over the sample holder and covered directly afterwards with another layer of thin film using sticky tape around the samples to make a tight 'sandwhich'. The synchrotron μXRF elemental imaging then took place within 15 min.

Data processing and statistical analyses

The data acquisition was handled by a custom workflow (Garrevoet 2025) and the XRF data were processed using non-linear least squares fitting as implemented in PyMCA (Solé et al. 2007). This produced 32-bit.tiff images with pixel values corresponding to μg cm^{-2} areal density of the element of interest. The figures were prepared in ImageJ (Schneider et al. 2012) by changing the lookup table (LUT) to 'Fire' and adjusting the pixel intensity value range with the levels slider such that background is scaled black and highest concentration values are scaled in the highest range of the LUT (nearly white). Finally, concentration scale bars using the 'calibration' tool and length scales were added.

Results

Zinc accumulation in field specimens

The roots and leaves of *C. waldsteinii* and associated rhizospheric soils were analysed and the mean and ranges of key elements are shown in Tables 1 and S1. The elemental concentrations in the soil samples

Table 1 Zinc concentrations in soil and plant samples of *Cardamine waldsteinii*. Data are expressed in µg g^{-1} as range and mean values. See Fig. 2 for the sampling point locations

Sample	Soil		Roots		Leaves	
	ranges	*means*	*ranges*	*means*	*ranges*	*means*
SP1	*n.a*	74.8	618–1310	860	1860–2560	2110
SP2	*n.a*	77.2	2080–4210	2870	3300–5650	4160
SP3	*n.a*	93.3	521–2450	955	721–3450	1430
SP4	*n.a*	108	562–1250	842	1390–4440	2990
SP5	*n.a*	99.9	697–1940	1160	2540–3640	2930
SP6	*n.a*	112	3250–6210	5170	1920–9260	7190
SP7	*n.a*	84.8	646–3080	2060	1140–5970	3490
SP8	165–240	184	1200–5810	3410	2320–9610	5530
SP9	117–165	146	1200–2210	1780	3240–5890	4980
SP10	78.9–137	110	*n.a*	*n.a*	1440–4370	2510
SP11	98.1–197	158	*n.a*	*n.a*	3120–7000	4580
SP12	27.4–89.9	73.5	*n.a*	*n.a*	1210–3260	2220
SP13	*n.a*	*n.a*	*n.a*	6090	1870–5220	3820

n.a.: data not available

varied in a similar range for all of the elements analysed, including Zn which ranged from 74 to 184 µg g^{-1}. The same applies to the plant samples, in which the trace elemental concentrations (with the exception of Zn) proved to be unremarkable (Table S1). Foliar Zn concentrations in *C. waldsteinii* individuals were up to > 9000 µg g^{-1} Zn and exceeded the hyperaccumulation threshold in almost all populations (except for SP1; Table 1) in at least one individual. Foliar Zn concentrations also exceeded those in the roots in all naturally grown populations (TF > 1), indicating a strong affinity for Zn translocation. This potential was confirmed by high values of the BCF, ranging from 15.3 (SP3) to 64.5 (SP6) (Table S2).

Elemental distribution in plant organs and tissues

The synchrotron µXRF elemental Zn maps of *C. waldsteinii* roots revealed predominant localisation in the main root, and a lower prevailing concentrations in the secondary roots. There was a non-distinct distribution of Zn in the root cortex, with a slightly higher Zn enrichment in the nodes of the lateral branches (Fig. 3). The epidermis was also an important localisation sites for Zn, but with a discontinuous distribution and higher concentrations in the proximal parts of the roots. Zinc accumulation in the epidermis was also observed in the root cross-section, but with significantly higher concentrations in the vascular bundles and endodermis, and some enrichment in the pericycle (Fig. 4A). In

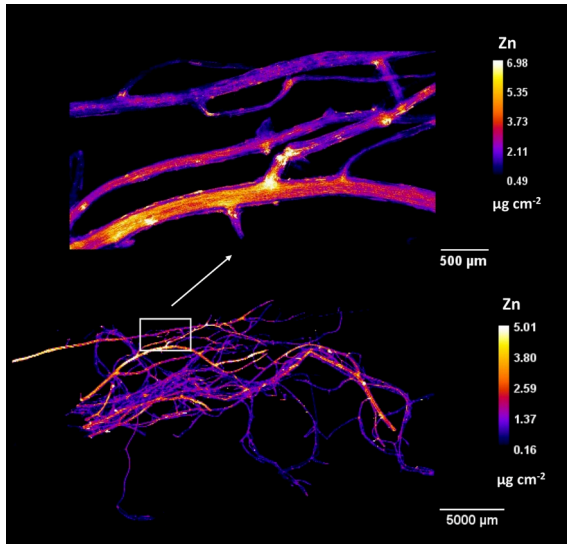

Fig. 3 Synchrotron µXRF elemental maps showing the distribution of Zn in intact roots of *Cardamine waldsteinii.* The elemental map was acquired at 5 µm (upper part) and 80 µm (lower part) step sizes with 5 ms (upper part) and 8 ms (lower part) dwell time per pixel. Scale and concentration bars are included.

the stem and petiole of *C. waldsteinii*, the epidermis had lower Zn concentrations (Fig. 4B and C). The pattern of Zn accumulation was the similar in the young and in the mature leaves of *C. waldsteinii*, with higher Zn concentrations in the old ones, and a clear Zn enrichment in the leaf margins, especially at the tip and around the distal veins (Fig. 5). In

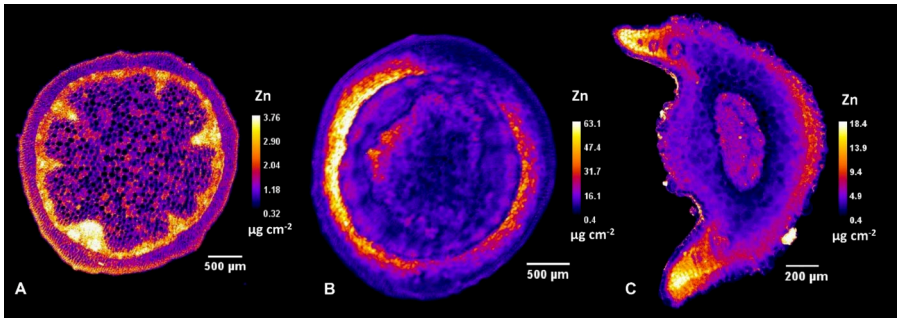

Fig. 4 Synchrotron µXRF elemental maps showing the distribution of Zn in root **A**, stem **B** and petiole **C** cross-sections of *Cardamine waldsteinii.* The elemental map was acquired at 10 µm **A**, 8 µm **B** and 2.5 µm **C** step sizes with 8 ms **A** and 5 ms **B**, **C** dwell time per pixel. Scale and concentration bars are included for each specimen.

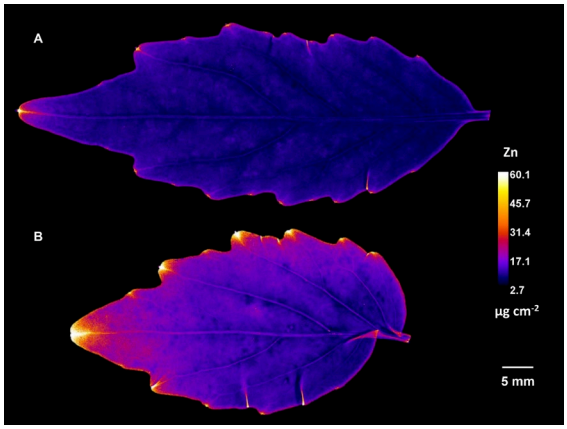

Fig. 5 Synchrotron µXRF elemental map showing the distribution of Zn in intact young **A** and mature **B** leaves of *Cardamine waldsteinii.* The elemental map was acquired at 33 µm step size with 7 ms dwell time per pixel. Scale and concentration bars are included.

mature leaves, Zn accumulation was also observed in the peripheral areas of the lamina, with higher prevailing concentrations in the distal parts.

Discussion

The elemental analysis of field collected samples of *C. waldsteinii* confirmed earlier herbarium findings about the potential for Zn hyperaccumulation in this species (Jakovljević et al. 2023). As *C. waldsteinii* can attain in excess of 9000 µg g^{-1} in its leaves, it clearly is a genuine Zn hyperaccumulator. Soil Zn concentrations were relatively low with subtle differences between the sampling sites due to the limestone-derived substrate. Consistently high foliar Zn concentrations when *C. waldsteinii* occurred on soils with < 240 µg g^{-1} Zn showed that hyperaccumulation is a constitutive trait in *C. waldsteinii*. This is akin the well-studied Zn hyperaccumulators *A. halleri* and *N. caerulescens* (Bert et al. 2000; Richau and Schat 2009).

The results of this study suggest preferential accumulation of Zn in the vascular bundles of the roots and stems of *C. waldsteinii*. Preferential accumulation of the hyperaccumulated element in the phloem is a feature in many different hyperaccumulator plant species (Lu et al. 2013; van der Ent et al. 2020). For essential elements such as Zn, this remobilisation is particularly important during plant growth, both for the supply of nutrients to young organs and for the removal of accumulated elements from the old leaves (Marschner 2012). Accumulation of Zn in the vascular bundles of the stem was also observed in *Sedum alfredii*, another hyperaccumulator of Zn, but only in the hyperaccumulating ecotype, whereas in non-hyperaccumulating ones the epidermis is the main site of accumulation (Tian et al. 2009). In the roots of the hyperaccumulating *S. alfredii* ecotype, the epidermis and cortex showed to be the main area of Zn accumulation (Gao et al. 2025). The localisation of Zn in the root and stem of *C. waldsteinii* is similar to the localisation of Zn and Ni in the Ni-hyperaccumulator *Noccaea tymphaea* (Hausskn.) F.K.Mey. (van der Ent et al. 2019). However, in contrast to the predominant accumulation around the secondary veins of *N. tymphaea*, Zn in the leaves of *C. waldsteinii* was mainly

localised in the marginal areas of the leaves. The accumulation of Zn in the marginal areas of the leaf with the highest concentrations in the leaf tips was also observed in *Sedum plumbizincicola* X.H.Guo & S.B.Zhou ex L.H.Wu (Jacquet et al. 2025), another hyperaccumulator of this element. Age-dependent differences in localisation and higher Zn concentrations were observed in the midrib and marginal areas of old leaves of *S. plumbizincicola* (Lu et al. 2014). This contrasts with *C. waldsteinii* where the accumulation of Zn occurs in the same foliar regions, only at different concentrations.

High values of bioaccumulation factors, indicative of a highly efficient Zn uptake even on soils with background concentrations of Zn, and a high leaf-to-root Zn ratio, suggest potential for in Zn biofortification, similar to how *C. hupingshanensis,* the Se hyperaccumulator, has already been extensively used for Se biofortification in China (Wang et al. 2024). Finally, this study highlights the need for a comprehensive study of the ionome of the species of the genus *Cardamine* (with over 200 species known worldwide) with the aim of discovering new metal/metalloid hyperaccumulator species.

Acknowledgements We acknowledge DESY (Hamburg, Germany), a member of the Helmholtz Association HGF, for the provision of experimental facilities. Parts of this research were carried out at PETRA III. Data was collected using beamline P06 operated/provided by DESY Photon Science. This research was supported in part through the Maxwell computational resources operated at Deutsches Elektronen-Synchrotron DESY, Hamburg, Germany. We would like to thank Dennis Brueckner for assistance in using beamline P06 and for performing the XRF data processing. We thank the Loki Schmidt Botanical Garden for donation of the *C. waldsteinii* specimen used in this study.

Author contributions SB and SŠ collected the samples in the field. MS prepared the samples and conducted the analysis. AvdE, KJ, MS and TM conducted the synchrotron µXRF experiment. KJ and AvdE wrote the first draft of the manuscript. All authors reviewed and approved the final draft of the manuscript.

Funding This work was supported by Ministry of Science Technological Development and Innovation of the Republic of Serbia (Grant Numbers 451–03-136/2025–03/200007 and 451–03-65/2024–03/200178) and by the Faculty of Agriculture, University of Zagreb.

Data availability The data that support this study will be shared upon reasonable request to the corresponding author.

Declarations

Conflicts of interest The authors declare no conflicts of interest relevant to the content of this manuscript.

References

Alloway BJ (2008) Zinc in Soils and Crop Nutrition, 2nd edn. International Zinc Association and International Fertilizer Industry Association, Brussels

Alloway BJ (2009) Soil factors associated with zinc deficiency in crops and humans. Environ Geochem Health 31(5):537–548. https://doi.org/10.1007/s10653-009-9255-4

Bert V, Macnair MR, De Laguerie P, Saumitou-Laprade P, Petit D (2000) Zinc tolerance and accumulation in metallicolous and nonmetallicolous populations of *Arabidopsis halleri* (Brassicaceae). New Phytol 146(2):225–233. https://doi.org/10.1046/j.1469-8137.2000.00634.x

Boesenberg U, Ryan CG, Kirkham R, Siddons DP, Alfeld M, Garrevoet J, Núñez T, Claussen T, Kracht T, Falkenberg G (2016) Fast X-ray microfluorescence imaging with submicrometer-resolution integrating a Maia detector at beamline P06 at PETRA III. J Synchrotron Rad 23:1550–1560. https://doi.org/10.1107/S1600577516015289

Broadley MR, White PJ, Hammond JP, Zelko I, Lux A (2007) Zinc in plants. New Phytol 173(4):677–702. https://doi.org/10.1111/j.1469-8137.2007.01996.x

Cappuyns V, Swennen R, Vandamme A, Niclaes M (2006) Environmental impact of the former Pb–Zn mining and smelting in East Belgium. J Geochem Explor 88(1–3):6–9. https://doi.org/10.1016/j.gexplo.2005.08.005

Gao Y, Yu H, Liu X, Lin H, Lu L (2025) Mechanisms involved in the positive effects of high zinc exposure on growth of *Sedum alfredii*. Plant Soil 507(1):823–843. https://doi.org/10.1007/s11104-024-06773-w

Garrevoet J (2025) A framework for data processing used at the hard X-ray micro/nano probe at PETRA III based on micro-services. J Phys Conf Ser 3010:012136. https://doi.org/10.1088/1742-6596/3010/1/012136

Jacquet J, Jakovljević K, Brueckner D, Sirguey C, van der Ent A (2025) Synchrotron elemental imaging reveals zinc distribution in the hyperaccumulator *Sedum plumbizincicola* (Crassulaceae). Ecol Res. In Press. https://doi.org/10.1111/1440-1703.70019

Jakovljević K, Mišljenović T, van der Ent A, Baker AJM, Andrejić G, Tomović G, Echevarria G (2023) Zinc (hyper) accumulation in *Cardamine waldsteinii*: from discovery in the herbarium to validation in the field. Plant Biosyst 157(4):851–857. https://doi.org/10.1080/11263504.2023.2204318

Kahlon PS, Kokkinopoulou P, Alfageme SB, Leong CK, Chen Z, Testerink C, van der Ent A (2024) Quantitative light element (sodium–calcium) profiling in plant tissues using monochromatic X-ray fluorescence analysis. bioRxiv 2024–10. https://doi.org/10.1101/2024.10.22.619597

Kaur H, Garg N (2021) Zinc toxicity in plants: a review. Planta 253(6):129. https://doi.org/10.1007/s00425-021-03642-z

Lu L, Tian S, Zhang J, Yang X, Labavitch JM, Webb SM, Latimer M, Brown PH (2013) Efficient xylem transport and phloem remobilization of Zn in the hyperaccumulator plant species *Sedum alfredii*. New Phytol 198(3):721–731. https://doi.org/10.1111/nph.12168

Lu L, Liao X, Labavitch J, Yang X, Nelson E, Du Y, Brown PH, Tian S (2014) Speciation and localization of Zn in the hyperaccumulator *Sedum alfredii* by extended X-ray absorption fine structure and micro-X-ray fluorescence. Plant Physiol Biochem 84:224–232. https://doi.org/10.1016/j.plaphy.2014.10.004

Marschner H (2012) Marschner's mineral nutrition of higher plants. Academic press, Elsevier

Paul AL, van der Ent A, Erskine PD (2019) Scandium biogeochemistry at the ultramafic Lucknow deposit, Queensland, Australia. J Geochem Explor 204:74–82. https://doi.org/10.1016/j.gexplo.2019.05.005

Reeves RD, Kruckeberg AR (2018) Re-examination of the elemental composition of some Caryophyllaceae on North American ultramafic soils. Ecol Res 33:715–722. https://doi.org/10.1007/s11284-017-1556-y

Reeves RD, Schwartz C, Morel JL, Edmondson J (2001) Distribution and metal-accumulating behavior of *Thlaspi caerulescens* and associated metallophytes in France. Int J Phytoremediation 3(2):145–172. https://doi.org/10.1080/15226510108500054

Reeves RD, Baker AJM, Jaffré T, Erskine PD, Echevarria G, van der Ent A (2018) A global database for hyperaccumulator plants of metal and metalloid trace elements. New Phytol 218:407–411. https://www.jstor.org/stable/90019919

Richau KH, Schat H (2009) Intraspecific variation of nickel and zinc accumulation and tolerance in the hyperaccumulator *Thlaspi caerulescens*. Plant Soil 314:253–262. https://doi.org/10.1007/s11104-008-9724-z

Sabovljević M, Tomović G, Djordjević V, Stanković S, Sabovljević A et al (2025) New records and noteworthy data of plants, algae and fungi in SE Europe and adjacent regions, 23. Compr Plant Biol 49(2):309–327. https://doi.org/10.2298/CPB2502309S

Schneider CA, Rasband WS, Eliceiri KW (2012) NIH image to ImageJ: 25 years of image analysis. Nat Methods 9(7):671–675. https://doi.org/10.1038/nmeth.2089

Solé VA, Papillon E, Cotte M, Walter Ph, Susini J (2007) A multiplatform code for the analysis of energy-dispersive X-ray fluorescence spectra. Spectrochim Acta B 62:63–68. https://doi.org/10.1016/j.sab.2006.12.002

Stein RJ, Höreth S, de Melo JRF, Syllwasschy L, Lee G, Garbin ML, Clemens S, Krämer U (2017) Relationships between soil and leaf mineral composition are element-specific, environment-dependent and geographically structured in the emerging model *Arabidopsis halleri*. New Phytol 213(3):1274–1286. https://doi.org/10.1111/nph.14219

Tian SK, Lu LL, Yang XE, Labavitch JM, Huang YY, Brown P (2009) Stem and leaf sequestration of zinc at the cellular level in the hyperaccumulator *Sedum alfredii*. New Phytol 182(1):116–126. https://doi.org/10.1111/j.1469-8137.2008.02740.x

van der Ent A, Baker AJM, Reeves RD, Pollard AJ, Schat H (2013) Hyperaccumulators of metal and metalloid trace elements: facts and fiction. Plant Soil 362(1–2):319–334. https://doi.org/10.1007/s11104-012-1287-3

van der Ent A, Spiers KM, Brueckner D, Echevarria G, Aarts MG, Montargès-Pelletier E (2019) Spatially-resolved localization and chemical speciation of nickel and zinc in *Noccaea tymphaea* and *Bornmuellera emarginata*. Metallomics 11(12):2052–2065. https://doi.org/10.1039/c9mt00106a

van der Ent A, de Jonge MD, Mak R, Mesjasz-Przybyłowicz J, Przybyłowicz WJ, Barnabas AD, Harris HH (2020) X-ray fluorescence elemental mapping of roots, stems and leaves of the nickel hyperaccumulators *Rinorea* cf. *bengalensis* and *Rinorea* cf. *javanica* (Violaceae) from Sabah (Malaysia), Borneo. Plant Soil 448:15–36. https://doi.org/10.1007/s11104-019-04386-2

Wang L, Li S, Wang F, Zhang N, Chen X, Wang X, He J, Cheng C, Zhu Z (2024) A se-hyperaccumulating plant *Cardamine violifolia*: from its nutritional value to potential applications in foods. Trends Food Sci Technol 154:104781. https://doi.org/10.1016/j.tifs.2024.104781

Zhang C, Charrois L, Jacquet J, Sirguey C, Chen Z, van der Ent A (2025) Monochromatic X-ray fluorescence spectroscopy for major and trace element analysis in plant science applications. Plant Soil. In Press. https://doi.org/10.1007/s11104-025-07984-5

Zhou Y, Tang Q, Wu M, Mou D, Liu H, Wang S, Zhang C, Ding L, Luo J (2018) Comparative transcriptomics provides novel insights into the mechanisms of selenium tolerance in the hyperaccumulator plant *Cardamine hupingshanensis*. Sci Rep 8(1):2789. https://doi.org/10.1038/s41598-018-21268-2